Research Article | Vol. 27, No. 20 | 30 Sep 2019 | OPTICS EXPRESS 29448
Optics EXPRESS

Analysis of enhanced-performance fibre Brillouin ring laser for Brillouin sensing applications

LEONARDO ROSSI,[1,2] DIEGO MARINI,[1] FILIPPO BASTIANINI,[3] AND GABRIELE BOLOGNINI[1,*]

[1]*Consiglio Nazionale delle Ricerche, IMM Institute, Bologna 40129, Italy*
[2]*University of Bologna, Bologna 40126, Italy*
[3]*Sestosensor s.r.l., Bologna 40069, Italy*
**bolognini@bo.imm.cnr.it*

Abstract: In this work, we present an enhanced design for a Brillouin ring laser (BRL), which employs a double resonant cavity (DRC) with short fiber length, paired with a heterodyne-based wavelength-locking system, to be employed as a pump-probe source for Brillouin sensing. The enhanced source is compared to traditional long-cavity pump-probe source, showing a significantly lower relative intensity noise (~-145 dB/Hz in the whole 0–800 MHz range), a narrow linewidth (10 kHz), and large tunability features, resulting in an effective pump-probe source in BOTDA systems, with an excellent pump-probe frequency stability (~200 Hz), which is uncommon for fiber lasers. The enhanced source showed an improved signal-to-noise ratio (SNR) of about 22 dB with respect to standard BRL schemes, resulting in an improved temperature/strain resolution in BOTDA applications up to 5.5 dB, with respect to previous high-noise BRL designs.

1. Introduction

Brillouin optical time domain analysis (BOTDA) has acquired a high degree of interest in the last few years, allowing for accurate measurements of strain and temperature along the length of an optical fiber [1]. BOTDA-based sensing systems rely on the stimulated Brillouin scattering (SBS) effect, which involves an optical pump lightwave signal amplifying a down-shifted counter-propagating probe [2]. The extent of the amplification depends on the pump-probe frequency shift and is maximum at the Brillouin frequency shift (BFS) value. Strain-temperature sensing is possible due to the dependence of BFS on these parameters at every point in the fiber [3]. In order to accurately reconstruct the BFS values along the sensing fiber, the pump-probe frequency shift must be accurately tuned and highly stable. This has commonly been accomplished through either optical sideband generation (OSB) methods [4], or by phase-locked loop (PLL) systems [5]. While these systems have proven to be highly performing, they generally require complex and expensive equipment: a wide bandwidth (~11 GHz) modulator and RF generator in the case of OSB, or two narrow linewidth tunable laser sources in the PLL case [6].

An attractive and cheaper alternative is represented by Brillouin ring lasers (BRLs), which employ stimulated Brillouin scattering to generate a downshifted Stokes signal through the interaction between an incident light (BRL pump) and the phonons in an optical fiber forming a ring cavity [7]. In the last years, BRL sources have been subject of investigation for their promising use in fields such as optical communication [8], radio over fiber [9,10] or as a distributed fiber sensor [11]. Since the shift between the pump and the Stokes signal is already in the range of the Brillouin frequency shift [6], it is possible to generate both pump and probe signals with a single source and tune their frequency shift using an electro-optic modulator (EOM) with a much narrower bandwidth than modulators used in the OSB method

#365477 https://doi.org/10.1364/OE.27.029448
Journal © 2019 Received 24 Apr 2019; revised 31 May 2019; accepted 16 Jun 2019; published 27 Sep 2019

Optics EXPRESS

[12]. In particular, such scheme allows for modulation with a bandwidth smaller than GHz value to span the Brillouin gain spectrum (BGS) of the sensing fiber, enabling a remarkable simplification of the electronics control circuitry and cost-reduction of the modulation system with respect to OSB based BOTDA sensors. It is also to note that, unlike in the PLL and OSB layouts, BRL resonators add a beneficial linewidth narrowing effect on the probe signal extracted from the cavity [13], which can be used to further improve BFS and consequently temperature/strain resolution [14]. A similar effect can be seen for the pump circulating inside the cavity, in particular when self-injection locking is applied [15], potentially leading to further improvements.

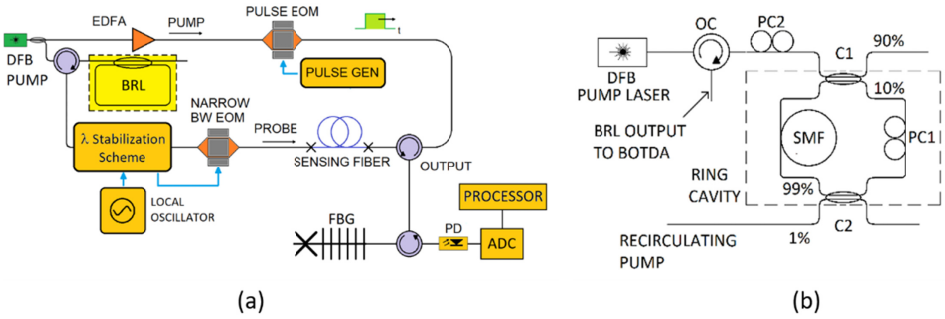

Fig. 1. Use of DRC-BRL (yellow) as dual pump-probe source in BOTDA system (a) and scheme of implemented doubly-resonant cavity Brillouin fiber ring laser (DRC-BRL) (b).

In order to improve BRL performance in BOTDA sensing systems it is essential to increase the pump-probe conversion efficiency and reduce its lasing threshold power, a goal that can be accomplished either by extending the interaction length through the employment of long cavity (LC) layout or by using a short cavity which is made simultaneously resonant for both pump and Stokes radiations (doubly-resonant cavity, DRC) [16]. The first option was explored in [17], where a LC-BRL (>100m long cavity) tunable over more than 200MHz was implemented in a BOTDA sensing scheme. However, it was also shown that, due to an inherent multi-mode cavity lasing, Stokes probe light coming from long cavities is characterized by a relatively large (~1 MHz) linewidth and high intensity noise, that in sensing applications can lead to constraints in terms of overall measurement accuracy (i.e. temperature/strain resolution). The second option is explored in this work, where we report the implementation of a BRL laser scheme that employs a few-meter long double resonant cavity (DRC) alongside a heterodyne-based wavelength locking system to further improve the signal stability. A similar doubly resonant short cavity approach was also explored in [15], where further stabilization of the BRL output was achieved through self-injection locking and [18], where for a similar purpose the short cavity was paired with a longer cavity and a FBG interferometer. Differently from the above mentioned solutions, the wavelength locking system presented here allows to simultaneously lock and accurately tune the pump-probe frequency shift by acting on the local oscillator frequency used in the locking circuit. The tunable probe light exhibits a low intensity noise (RIN ~-145 dB/Hz in the 0-800 MHz range), a narrow linewidth (10 kHz) and an exceptional pump probe stability (~200Hz) which is uncommon for fiber lasers, resulting in a stable and efficient pump-probe source for BOTDA sensor systems.

2. Double resonant cavity (DRC)

In BOTDA systems, in order to accurately reconstruct the Brillouin gain spectrum along the sensing fiber and evaluate the BFS providing temperature/strain information, it is necessary to tune the pump-probe frequency shift with high accuracy and to ensure that such shift will remain stable for the duration of the measurement. In addition, the stability of the optical

Optics EXPRESS

probe directly influences the frequency resolution for the BFS, which, in its turn, determines both temperature and strain resolution [19,20].

The scheme of a BOTDA system employing our DRC-BRL and the stabilization scheme is shown in Fig. 1(a). The pump and probe are generated by the same DFB laser source (λ = 1553.26 nm, 350 kHz wide linewidth). In the pump branch, the DFB seed is amplified through an erbium-doped fiber amplifier (EDFA) and pulsed by an electro-optic modulator (EOM). In the probe branch, the BRL generating the tunable probe light is coupled into the λ-stabilization scheme described below and modulated by a low-bandwidth EOM. The stabilization scheme (explained below in detail) is used to lock the probe to the pump signal and tune their frequency shift over a range of frequencies. The Standard BOTDA traces are then obtained by acquiring the detected amplified probe light intensity through a PIN photodiode and a fast analog-to-digital-converter (ADC) with the subsequent data processing to reconstruct the Brillouin Gain Spectrum (BGS). The Stokes signal is selected through reflection by a fiber Bragg grating (FBG) filter (also reducing unwanted noise and and improving SNR of BOTDA traces as explained below in section 3.4) and a second optical circulator than couples it into the PIN photodiode. The FBG used in the set-up has a 6 GHz large 3dB reflection bandwidth.

The structure of the BRL is shown in Fig. 1(b): two optical couplers are used to define a fiber ring. Through one of the couplers (C1), the light from the laser pump is injected into the ring. Once the light circulating inside the cavity reaches a given intensity threshold, a counter-propagating and frequency downshifted optical signal (Stokes light) is generated and amplified by Stimulated Brillouin Scattering (SBS), and then amplified through multiple loop propagation inside the ring, further increasing intensity and narrowing its linewidth. The Stokes output is then coupled out through C1 and inserted into the BOTDA through an optical circulator (OC).

More in detail, in the DRC-BRL shown in Fig. 1(b), the pump is provided by a frequency stabilized DFB laser whose operating wavelength matches the ring resonant frequency and is coupled to an optical circulator (OC) and then, through an optical coupler (C1), enters the fiber ring cavity, which is given by a single-mode fiber spool (SMF) (< 10 m length). The BFS value of the fiber employed in the ring lies below 10 GHz so that, as will be described in the following sections, only the lower frequency side-band signal generated by the wavelength-locking scheme modulator lies within the BGS of the sensing fibers that commonly show BFS values ~10.6 GHz. The ring fiber is thermally stabilized within a laboratory case and located on an active vibration isolating table in order to reduce acoustic noise and thermal fluctuations that are typically responsible for low-frequency (<100 kHz) intensity and phase noise in fiber ring laser signals. To ensure optimal polarization coupling between pump and Stokes lightwaves, which is necessary to maximize SBS gain, two polarization controllers (PC1 and PC2) are used before the ring and inside it respectively. The counter-propagating (counterclockwise) Stokes light from the ring cavity is coupled out from the 3rd port of OC as the BRL output. A second optical coupler (C2) allows to monitor both re-circulating pump and Stokes. When BRLs are used as pump-probe sources, the Stokes signal is subject to both intensity and phase noise which can degrade the overall performance [21]; in particular, the frequency noise in the Stokes signal is influenced by the so-called mode hopping. A schematic representation of the mode hopping effect is given in Fig. 2. In mode hopping, thermal noise and vibrations alter the cavity free spectral range (FSR), causing a shift in the dominant lasing mode [22].

Optics EXPRESS

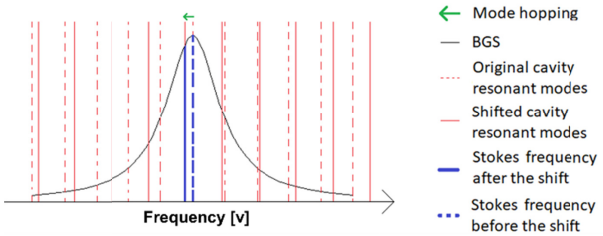

Fig. 2. Mode hopping after changes in resonant modes in the cavity due to shifts in length.

A way to effectively suppress mode hopping and multi-mode lasing is to make sure that one cavity resonant mode is spectrally lying inside the BGS [15]. This is achieved by reducing the ring resonator length until the free spectral range becomes larger than the Brillouin gain bandwidth. The FSR is given by:

$$FSR = \frac{c}{n \cdot L} \tag{1}$$

where c is the speed of light in the void, n is the fiber refractive index and L is the fiber cavity length.

In order to achieve an ultra-narrow bandwidth pump-probe source and improved sensing performance, we implemented a single-mode double resonant cavity (DRC) BRL. In a double resonant cavity, the Stokes output is suppressed unless the pump frequency value and the downshifted frequency shift both fall on resonant modes for the cavity. This is implemented by designing the ring in such a way that the pump frequency is in resonance and the BFS value coincide with an integer number of the FSR [23]:

$$\frac{2nV_a}{\lambda} = k \cdot FSR = k\frac{c}{nL} \tag{2}$$

where k represents any integer value, V_a is the acoustic wave velocity along the fiber and λ is the pump wavelength. In order to obtain a doubly-resonant cavity we carefully selected the ring length using the single cut technique demonstrated in [23]. The pump wavelength λ_L^k that satisfies the double resonance condition for a given cavity of length L and order k is:

$$\lambda_L^k = \frac{1}{k}\frac{2n^2V_a}{c}L \tag{3}$$

By localizing two consecutive peaks, it is possible to measure the mode order k through the formula:

$$k = \frac{\lambda_L^k}{\lambda_L^{k-1} - \lambda_L^k} \tag{4}$$

It can be shown that the excess length to be removed from a cavity in order to move a doubly-resonant peak of order k at λ_L^k to a new peak of order j at λ_{LM}^j is given by [24]:

$$\Delta L = \frac{c\lambda_L^k}{2n^2V_a}\left(k\frac{\lambda_{LM}^j}{\lambda_L^k} - k\right) \tag{5}$$

From Eq. (3), it is also possible to find out the wavelength separation between consecutive modes, defined as $\Delta\lambda_{DRC}^k = \lambda_L^k - \lambda_L^{k+1}$:

Optics EXPRESS

$$\Delta\lambda_{DRC}^{k} = \left(\frac{1}{k} - \frac{1}{k+1}\right)\frac{2n^2V_a}{c}L = \frac{1}{k(k+1)}\frac{2n^2V_a}{c}L \tag{6}$$

which is equivalent to a frequency separation of

$$\Delta\nu_{DRC} = \frac{c \cdot FSR}{2n \cdot V_A} = \frac{c^2}{2n^2V_A} \cdot \frac{1}{L} \tag{7}$$

From Eqs. (3) and (6), noting that the double resonant mode order is roughly proportional to the cavity length, an inverse relation can be found between $\Delta\lambda_{DRC}^{m}$ and cavity length L.

In order to measure the mode frequency separation between doubly resonant modes in our BRL and calculate the excess length ΔL we used a tunable laser (1550-1560 nm) to measure the output BRL intensity, said Brillouin response, as a function of the pump wavelength for different cavity lengths (from 10 m down to 4 m). In Fig. 3(a) we reported the output BRL Stokes power as a function of pump wavelength for a cavity length of approximately 5 m. In Fig. 3(a), the presence of intensity peaks followed by lower intensity regions clearly shows the double resonant mode patterns (peak separation ~5 nm). Through such measurements, it was possible to plot the doubly resonant mode peak separation in nm as a function of the cavity length. The results are shown in Fig. 3(b). The inversely proportional relation was also verified by performing a least squares power curve fit on the data on the graph, which gave a best fit exponent of −1.032 (close to the expected −1 value) and a R^2 value of 0.9966. The used length values are short enough to ensure that only one of the cavity resonant modes lies within the BGS: for ring length values < 10 m the FSR from Eq. (1) is larger than the linewidth of the BGS (~20 MHz). Then, to make sure that the DRC-BRL with the DFB pump wavelength used for BOTDA applications (λ = 1553.26 nm, 350 kHz linewidth) satisfies the double resonance condition, we removed the excess length calculated through Eq. (5) obtaining a final length of 3.4 m. Once double resonance was achieved, both pump and Stokes signals are resonantly amplified in this scheme, leading to a strong enhancement of power transfer from pump to the Stokes (probe) signal. The doubly resonant SC-BRL shows a lasing threshold power of approximately 10 dBm and an extracted power of 1,5 mW (in correspondence to a DFB pump power of about 14 dBm), that is adequate for use as a probe signal in BOTDA applications.

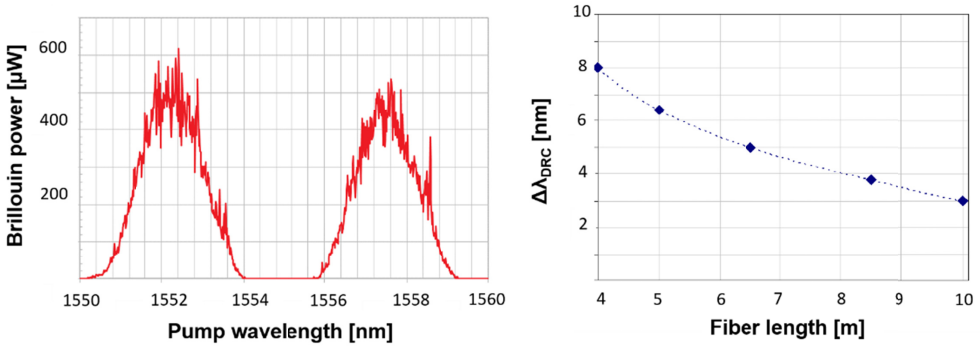

Fig. 3. BRL Stokes power as a function of DFB pump wavelength for a cavity length of 5 m (a) and doubly resonant wavelength peak separation versus cavity fiber length in DRC-BRL (b).

Optics EXPRESS

3. Wavelength locked DRC-BRL

One of the issues of practical DRC-BRL is that while fluctuations of the cavity length induced by environmental vibrations and thermal instabilities no longer cause mode hopping, they can still detune the pump resonance reducing overall lasing stability [21] alongside the combination of Kerr effect and mode pulling [22]. DRC-BRL lasing can be stabilized by a variety of techniques such as those that use feedback systems locking the cavity length [25] or the pump wavelength [26]. To counteract the detuning effect, improve the pump-probe frequency shift stability and reduce the intensity noise, we employed an active DRC-BRL lasing wavelength locking system which also succeeds at compensating frequency drift, further improving the frequency-shift noise.

3.1. Wavelength locking scheme

The employed scheme is depicted in Fig. 4. From the DRC-BRL described in Section 2, small fractions of both output pump and BRL Stokes lightwaves are redirected by two optical couplers (S1 and S2) into the 3-dB optical coupler S3, and their combined beating signal Δf_{BRL} is converted into an RF tone by a fast photo-detector (PD). A harmonic mixer is used to mix the RF tone at the pump-Stokes frequency difference ($\Delta f_{BRL} = f_{pump}-f_{BRL} < 10$ GHz) with the signal from a tunable local oscillator whose frequency (f_{LO}) is always kept higher than Δf_{BRL} ($f_{LO} > \Delta f_{BRL}$, in our experiment $f_{LO} = 10.7$-11.5 GHz); two sidebands ($f_{LO} \pm \Delta f_{BRL}$) are resulted from harmonic mixing. A low-pass filter removes the (unwanted) upper sideband, while the frequency-difference RF component ($f_{LO}-\Delta f_{BRL}$), which in our experiment is lying in the 100-900 MHz range, is used to drive a slow (<1 GHz bandwidth) Mach-Zehnder electro-optical modulator (EOM). Corresponding optical sidebands are thus generated in modulation of Stokes light by EOM, while a suitable biasing of the EOM ensures efficient suppression of the (Stokes) carrier (>20 dB suppression). Of the two sidebands in the modulated Stokes light, the frequency of the lower sideband ($f_{LSB} = f_{BRL} - f_{LO} + \Delta f_{BRL} = f_{pump} - f_{LO}$) is shifted from the pump by the frequency of the tunable oscillator f_{LO}. This way, it is possible to tune the pump-probe frequency shift from the initial Δf_{BRL} automatically provided by the BRL to the values required to span the whole BGS of the sensing fiber. Since the BRL signal frequency < 10 GHz does not lie within the gain spectrum of the sensing fibers that are commonly employed, the upper sideband signal that is generated by the EOM does not interact with the pulsed pump in the BOTDA set-up and does not have to be suppressed. In addition, any frequency perturbation in the ring, which would change the BRL output to $f_{BRL} = f_{BRL} + \delta f$, would also lower the Δf_{BRL} by $-\delta f$, causing the frequency that is fed into the EOM to change from ($f_{LO}-\Delta f_{BRL}$) to $f_{LO}-(\Delta f_{BRL}-\delta f)$, resulting in a modulation change of exactly δf. This would result in a perturbed lower sideband frequency equal to $f_{LSB} = f_{BRL} + \delta f - f_{LO} + \Delta f_{BRL} - \delta f = f_{pump} - f_{LO}$. This means that every perturbation in the BRL cavity is effectively compensated by the EOM, leaving the final pump-probe frequency shift unalterated. It's worth noting that OSB technique employs modulators having bandwidth >10-11 GHz to directly modulate the probe signal from the pump frequency values to those required to span the BGS of the sensing fiber.

Optics EXPRESS

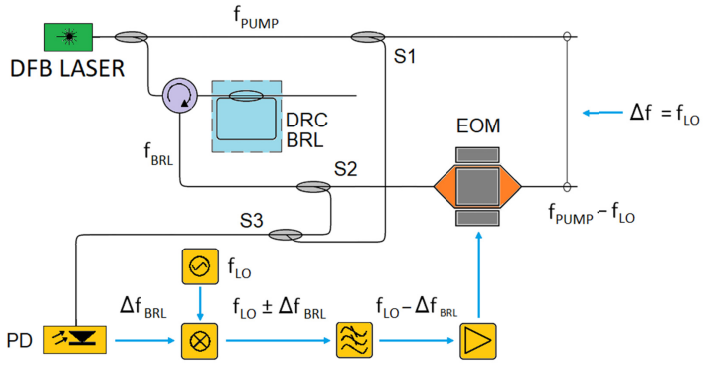

Fig. 4. Scheme of implemented active wavelength locking technique for DRC-BRL.

3.2. Frequency stability characterization

In order to verify the performance of the wavelength locking scheme in BOTDA, the stability of the pump-frequency shift was evaluated in terms of linewidth, frequency stability and intensity noise. The spectrum of the pump-probe beating signal was thus measured (choosing a local oscillator frequency f_{LO} = 10.86 GHz) using a 12 GHz bandwidth photodetector; the resulting RF tone was then recorded by an Electrical Spectrum Analyzer (ESA). In Fig. 5 the acquired spectra are reported. The spectral acquisition was time-averaged over two different timescales: 10 ms (left), which is comparable to the duration of a single BOTDA measurement, and 120 s (right). For the 10 ms timescale, the full width half maximum (FWHM) is ~200 Hz; the FWHM for longer interpolation times at 120 s results to be of the same order of magnitude at ~400 Hz. Both results show that the pump-locked probe signal can be highly stable in the BOTDA measurement, both in the single measurement timescale and on the longer averaged-trace timescale.

Similar linewidths were obtained for different frequency shifts, spanning the entire local oscillator range (10.7-11.5 GHz) showing that the wavelength stabilization scheme, combined with the DRC-BRL, is capable to provide both a narrow linewidth and reliably tunable pump-probe source.

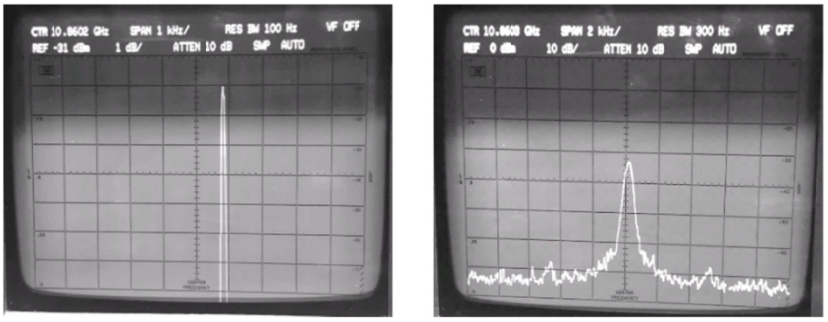

Fig. 5. Electrical spectrum of pump-probe beating for stabilized DRC-BRL with 10 ms (left) and 120 s (right) measurement time. The frequency range is centered at the local oscillator frequencies f_{LO} 10.8602 GHz that is fed into the active wavelength-locking scheme. The y axis scale is 1dB/division (left) and 10 dB/division (right) and x axis scale is 1 kHz/division (left) and 2 kHz/division (right).

In addition to the above-mentioned pump-probe frequency stability which is essential for assessing application of DRC-BRL to BOTDA systems, we also measured the absolute BRL linewidth, thus evaluating the narrowing effect of the short-cavity double resonant BRL. We hence employed the self-heterodyne method [12] to measure the absolute spectral linewidth

Optics EXPRESS

of the probe lightwave. A Mach-Zehnder interferometer with a 12 km long fiber delay line in one arm and a 150 MHz acusto-optic modulator in the second arm is used for this purpose with a fast (12 GHz bandwidth) photodetector and ESA for the analysis of the beat signal. The optical path difference between the two arms allows to measure signal having spectral linewidth values down to about 6 kHz [27]. The attained full width at half maximum (FWHM) of the spectrum for signal power of 0.75 mW, pump power of 12.6 dBm and ~200 μW extracted from the Mach-Zehnder intereferometer (shown in Fig. 6) results to be ~10 kHz, thus significantly narrower than the original DFB laser linewidth (350 kHz). The observed narrowing of the Stokes signal is due to the combined influence of the acoustic damping and the cavity feedback of the ring resonator [13]. The expected Stokes spectral linewidth value $\Delta\nu_S$, considering situations with FSR values comparable to the BGS bandwidth, that is the case of short-cavity layout, is given by [13]

$$\Delta\nu_S = \frac{\Delta\nu_P}{1+\frac{\pi\Delta\nu_B}{\Gamma}} \tag{8}$$

where $\Delta\nu_p$ is the pump linewidth, $\Delta\nu_B$ is the Brillouin linewidth. Γ is a parameter depending on the length L and coupling ratio of the cavity R and is defined as: $\Gamma = c/nL\ln R$. Using the experimental values of the used BRL cavity, we obtained an expected Stokes linewidth approximately of 5 kHz which is in line with self-heterodyne measurements. Outside the frequency range reported in Fig. 5, the signal is within the noise due to the SNR of the measurement set-up, which limited the measure sensitivity to about −80 dBm; however, the attained power levels were 20dB below the peak values, and no additional peaks were observed. Furthermore, we have performed spectral linewidth measurements on BRL signal with different input pump power values above the laser threshold; in particular, we have carried out measurements of the BRL signal with power ranging from 0.5 to 1.2 mW and no significant variations of the spectral linewidth values have been observed.

One notable advantage of this active stabilization scheme is that, thanks to the removal of the noisy fluctuation and the optical filtering provided by the DRC-BRL cavity, the Stokes light exhibits a linewidth that is narrower than the original DFB pump laser. Moreover, as described above, in this scheme the anti-Stokes sideband, which is represented by the upper sideband created by the modulator, has frequency of $f_{USB} = f_{BRL} + f_{LO} - \Delta f_{BRL}$ which does not lie within the Brillouin sensing region (unlike e.g. direct DFB modulation used in standard OSB methods) and thus it doesn't need to be filtered out, allowing for simpler detection schemes. In addition, since the output from the BRL cavity is especially close to the pump-probe frequency shift, the EOM only needs to tune/modulate at a frequency $f_{LO} - \Delta f_{BRL}$, which is in the range of 100 to 900 MHz for very large tuning ranges. This means that it is possible to employ a slower-response EOM (hundreds of MHz) compared to the faster EOMs needed in direct modulation schemes (>10 GHz bandwidth). Finally, the re-circulating pump extracted from the Brillouin ring laser cavity experiences a similar filtering effect as the DRC-BRL Stokes light. The proposed scheme hence allows us for a wide, stable tuning of the frequency shift that is expected to allow for an accurate reconstruction of the Brillouin gain spectrum in BOTDA, as it will be shown in the next section. Please note that the wavelength locking scheme circuitry can be easy implemented using commercial low-cost electronic components.

Optics EXPRESS

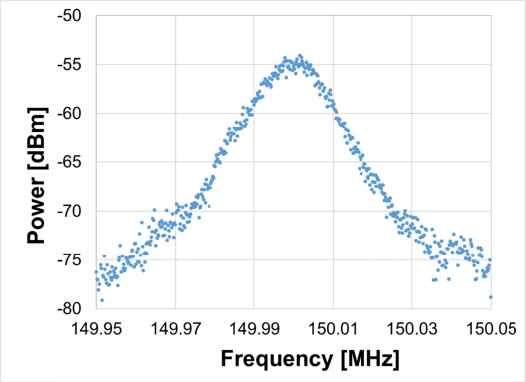

Fig. 6. DRC-BRL linewidth obtained through delayed self-heterodyne technique.

3.3. Intensity noise measurements

In addition to the frequency stability, an assessment of the intensity noise of the actively stabilized DRC-BRL source was carried out. Generally speaking, fiber lasers are expected to exhibit larger fluctuations and reduced stability with respect to integrated diodes, due to the longer cavity lengths, which give rises to typical effects such as cavity mode hopping and pump-signal noise transfer [26]. In order to evaluate the effects of short cavity and active stabilization for our BRL, characterization of relative intensity noise (RIN) was carried out for the stabilized DRC-BRL and the standard long cavity (~2 km) BRL developed in [12], as well as the pump DFB. The RIN is defined as the power spectral density of the time-varying signal power fluctuations $\delta P(t)$ [27]:

$$RIN(\omega) = \frac{1}{\bar{P}^2}\int \langle \delta P(t)\delta P(t+\tau)\rangle \exp(-i\omega\tau)\, d\tau \qquad (9)$$

where $\bar{P}$ is the average of the optical power and <·> denotes the ensemble average (over a large number of measurements). RIN measurements were carried out on the BRL and DFB light using a fast p-i-n photodetector (InGaAs-based, 11 GHz bandwidth), using an electrical spectrum analyser (working up to 15 GHz) to acquire the power spectrum $\delta^2(\omega)$ and subtracting thermal and shot noise terms [28].

The results of the RIN spectral measurements up to 800 MHz for the wavelength-locked BRL, free-running long-cavity (~2km) BRL and DFB pump are reported in Fig. 7. From Fig. 7, it can be noted that in the standard long-cavity BRL higher RIN values are observed in the low frequency range (0-400 MHz), while the actively stabilized DRC-BRL exhibits lower RIN across the entire frequency range. In particular, while for standard BRL the low-frequency maximum RIN values are about −90 dB/Hz (in the 10-15 MHz frequency range), the RIN levels of stabilized DRC-BRL scheme are only slightly above the original pump DFB levels, i.e. between −140 dB/Hz and −150 dB/Hz across the whole 1-800 MHz range. On the other hand, RIN values beyond 500 MHz frequencies appear low even for the standard BRL and remain approximately constant with an average value of about −145 dB/Hz. In the low frequency spectral region (1-50 kHz), as shown in the inset of Fig. 7, the measured RIN levels were higher than in the MHz range, but still limited below ~-100 dB/Hz. From these results it becomes evident how the short together with the stabilization techniques, succeeds not only in stabilizing the frequency shift, but also in improving the standard BRL intensity noise values that are typically known to exhibit higher RIN values with respect to diode laser pump seed, especially at lower frequencies [29].

Optics EXPRESS

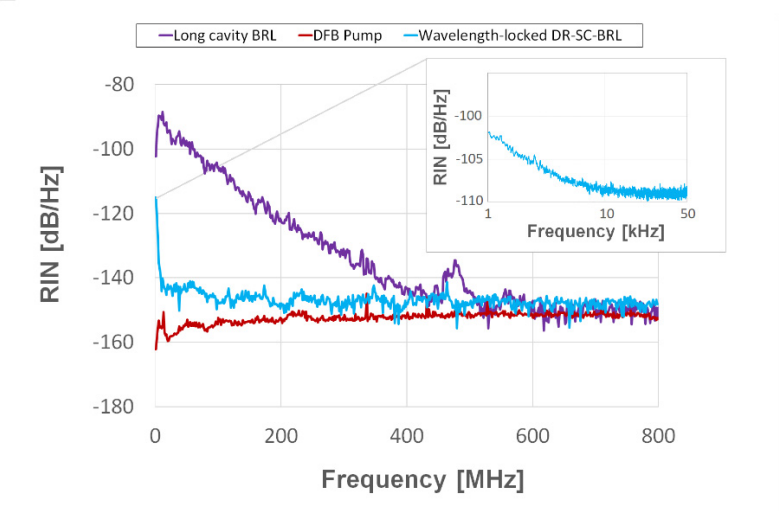

Fig. 7. Measured spectral RIN characteristics for the standard BRL, for λ-locked DRC-BRL and for pump DFB laser. Inset: RIN measurement for DRC-BRL in the 1-50 kHz frequency range.

3.4. SNR improvement in BOTDA applications

By evaluating the signal to noise ratio (SNR) of the probe signal in BOTDA applications, it is possible to provide a quantitative estimate on the effect of the potential SNR improvement thanks to reduced RIN that would arise by using the DRC-BRL instead of the LC-BRL as the probe source for a BOTDA sensor. In a typical BOTDA configuration (refer to Fig. 1(a)), the SNR of the detected probe signal at the photodetector can be expressed as [1]:

$$SNR = \frac{I_S}{\delta} = \frac{I_S}{\sqrt{\delta_{th}^2 + \delta_{sh}^2 + \delta_{sp-sp}^2 + \delta_{sp-s}^2 + \delta_{RIN}^2}} \tag{10}$$

where I_S is the current generated by the photodetector, and δ_{th}^2, δ_{sh}^2, δ_{sp-sp}^2, δ_{sp-s}^2, δ_{RIN}^2 are the noise variances given respectively by thermal noise and shot noise of the photodetector, spontaneous-spontaneous and signal-spontaneous beat noise of the EDFA and the RIN of the optical probe. Note that the FBG placed at receiver side contributes removing out-of-band light noise sources possibly impairing the SNR (e.g. ASE from EDFA and related ASE-signal beat noise, Rayleigh back-scattered pump light etc). The 3 dB bandwidth of FBG (6 GHz) was large enough to keep the Stokes signal frequency far from the slope of FBG reflection spectrum (thus also limiting the possible noise contributions generated by the phase-to-intensity conversion of signal phase noise due to thermal drift of the FBG bandwidth).

Unlike with probes from most low-RIN sources, where the main limit to the SNR is due to the spontaneous-signal beat noise δ_{sp-s}^2, in probe signals generated by a noisy fiber ring laser the most important contribution is given by the RIN [30]. The SNR, together with the Brillouin linewidth $\delta\nu_B$, determines the minimum detectable frequency shift of the reconstructed Brillouin gain spectrum fit for the acquired BOTDA trace at a given fiber location. Actually, the frequency resolution in BFS measurements on standard BOTDA systems can be found using the following expression:

$$\delta\nu_B = \frac{\Delta\nu_B}{\sqrt{2}\,(SNR)^{\frac{1}{4}}} \tag{11}$$

Optics EXPRESS

and from this value it is hence easy to estimate corresponding temperature and strain resolutions, which are respectively given by [31]:

$$\delta T = \frac{\delta \nu_B}{C_T \nu_B(t_r)} \qquad \delta \varepsilon = \frac{\delta \nu_B}{C_S \nu_B(0)} \tag{12}$$

where C_T and C_S are the linear temperature and strain coefficients, respectively, while $\nu_B(t_r)$ and $\nu_B(0)$ represent Brillouin frequency shifts of sensing fiber at reference temperature and of unstrained sensing fiber, respectively [31].

It is hence possible to provide an estimation of attainable resolution improvements for BOTDA applications by using a wavelength-locked DRC-BRL instead of a higher-RIN LC BRL. In the following analysis, the major noise source is assumed to be given by the laser RIN, and other noise sources (see Eq. (10)) are considered of smaller extent with respect to the laser intensity fluctuations. Clearly, while this approach is valid only with noisy laser sources such as fiber lasers (as for our BRL), it gives a good estimation about whether the BRL intensity noise can be a limiting parameter for BOTDA applications.

The resulting probe SNR due to source intensity fluctuations (SNR_{RIN}) has actually been calculated by integrating the measured RIN values over the BOTDA receiver bandwidth (125 MHz). This resulted in a SNR_{RIN} of ~38.7 dB for the standard long-cavity BRL, and of ~61 dB for the λ-locked DRC-BRL. The short-cavity double-resonance λ-locked BRL scheme hence allows a notable SNRRIN improvement of ~22.3 dB.

Referring to the BOTDA set-up shown in Fig. 1(a), and to the details and results of experiments reported in [12] for the standard BRL configuration, it is hence possible to infer the SNR and resolution improvements attained by using the new DRC-BRL scheme. Actually, it can be easily seen from Eqs. (10)–(12) (in the assumption of RIN as the prevalent component in probe fluctuations and in detected SNR), that the resolution improvement (in terms of frequency, temperature or stain resolution) achievable with the DRC-BRL can reach a value up to 5.5 dB.

4. Conclusions

In conclusion, we reported on an enhanced performance fiber Brillouin ring laser (BRL) exploiting a doubly resonant cavity (DRC) using a short single-mode fiber length, combined with an optical wavelength locking technique based on heterodyne detection. The novel DRC-BRL configuration has shown to provide a highly stable and tunable probe light, which can be highly suitable for BOTDA sensing applications. The probe source intensity noise characterization showed a measured RIN of ~-145 dB/Hz across the whole 0-800 MHz range; the measured laser linewidth resulted to be only 10 kHz, and an excellent pump-probe frequency stability was observed (pump-probe stability was 200 Hz with 10 ms integration time and 400 Hz with 120 s integration time). It's worth noting that, unlike in the PLL and OSB layouts, BRL resonators add a beneficial linewidth narrowing effect on the probe signal extracted from the cavity which can be used to further improve BFS and consequently temperature/strain resolution. The DRC-BRL light showed an improved intensity-noise signal-to-noise ratio (SNR) of about 22.3 dB with respect to standard BRL schemes, resulting in improved temperature/strain resolutions in BOTDA applications up to 5.5 dB with respect to previous high-noise BRL designs. The carried out analysis then indicates that stabilized DRC-BRL could be successfully employed as dual pump-probe source in accurate Brillouin optical time-domain sensor system applications, as an efficient and cost-effective alternative to the solutions based on PLL and OSB techniques, with a narrow linewidth (10 kHz) and an exceptional pump probe stability (~200Hz) which is uncommon for fiber lasers.

Optics EXPRESS

Funding

European Union through Horizon 2020, the Framework Programme for Research and Innovation, under project PULSe (737801).

References

1. M. A. Soto and L. Thévenaz, "Towards 1'000'000 resolved points along a Brillouin distributed fibre sensor," Proc. SPIE **9157**, 9157–9685 (2014).
2. C. A. Galindez-Jamioy and J. M. Lopez-Higuera, "Brillouin distributed fiber sensors: an overview and applications," J. Sens. **2012**, 1–17 (2012).
3. T. Kurashima, T. Horiguchi, and M. Tateda, "Distributed-temperature sensing using stimulated Brillouin scattering in optical silica fibers," Opt. Lett. **15**(18), 1038–1040 (1990).
4. M. Niklès, L. Thevenaz, and P. A. Robert, "Simple distributed fiber sensor based on Brillouin gain spectrum analysis," Opt. Lett. **21**(10), 758–760 (1996).
5. T. Kurashima, T. Horiguchi, and M. Tateda, "Distributed-temperature sensing using stimulated Brillouin scattering in optical silica fibers," Opt. Lett. **15**(18), 1038–1040 (1990).
6. F. Bastianini, D. Marini, and G. Bolognini, "Modified Brillouin ring laser technology for Brillouin-based sensing," Proc. SPIE **9634**, 9634E (2015).
7. D. Marini, L. Rossi, F. Bastianini, and G. Bolognini, "Enhanced-performance fibre Brillouin ring laser for Brillouin sensing applications," in *Optical Fiber Sensors, OSA Technical Digest* (Optical Society of America, 2018), paper ThE71.
8. Y. Liu, M. Zhang, J. Zhang, and Y. Wang, "Single-longitudinal-mode triple-ring Brillouin fiber laser with a saturable absorber ring resonator," J. Lit. Technol. **35**(9), 1744–1749 (2017).
9. Y. Liu, M. Zhang, P. Wang, L. Li, Y. Wang, and X. Bao, "Multiwavelength single-longitudinal-mode Brillouin–erbium fiber laser sensor for temperature measurements with ultrahigh resolution," IEEE Photonics J. **7**(5), 1–9 (2015).
10. Y. Liu, J. L. Yu, W. R. Wang, H. G. Pan, and E. Z. Yang, "Single longitudinal mode Brillouin fiber laser with cascaded ring Fabry–Pérot resonator," IEEE Photonic Tech. L. **26**(2), 169–172 (2014).
11. Z. Ou, X. Bao, Y. Li, B. Saxena, and L. Chen, "Ultranarrow linewidth Brillouin fiber laser," IEEE Photonic. Tech. L. **26**(20), 2058–2061 (2014).
12. D. Marini, M. Iuliano, F. Bastianini, and G. Bolognini, "BOTDA sensing employing a modified Brillouin fiber laser probe source," J. Lightwave Technol. **36**(4), 1131–1137 (2018).
13. A. Debut, S. Randoux, and J. Zemmouri, "Linewidth narrowing in Brillouin lasers: Theoretical analysis," Phys. Rev. A **62**(2), 023803 (2000).
14. A. Minardo, R. Bernini, and L. Zeni, "Analysis of SNR penalty in Brillouin optical time-domain analysis sensors induced by laser source phase noise," J. Opt. **18**(2), 025601 (2016).
15. V. V. Spirin, C. A. López-Mercado, P. Mégret, and A. A. Fotiadi, "Single-mode Brillouin fiber laser passively stabilized at resonance frequency with self-injection locked pump laser," Laser Phys. Lett. **9**(5), 377–380 (2012).
16. L. F. Stokes, M. Chodorow, and H. J. Shaw, "All-fiber stimulated Brillouin ring laser with submilliwatt pump threshold," Opt. Lett. **7**(10), 509–511 (1982).
17. M. Iuliano, D. Marini, F. Bastianini, and G. Bolognini, "BOTDA sensing system employing a tunable low-cost Brillouin fiber ring laser," in *Proceedings of Optical Fiber Sensors Conference* (IEEE, 2017), pp. 1–4.
18. V. V. Spirin, C. A. López-Mercado, D. Kinet, P. Mégret, I. O. Zolotovskiy, and A. A. Fotiadi, "A single-longitudinal-mode Brillouin fiber laser passively stabilized at the pump resonance frequency with a dynamic population inversion grating," Laser Phys. Lett. **10**(1), 0151021 (2012).
19. J. Urricelqui, M. A. Soto, and L. Thévenaz, "Sources of noise in Brillouin optical time-domain analyzers," Proc. SPIE **9634**, 963434 (2015).
20. M. A. Soto and L. Thévenaz, "Modeling and evaluating the performance of Brillouin distributed optical fiber sensors," Opt. Express **21**(25), 31347–31366 (2013).
21. P. Nicati, K. Toyama, and H. J. Shaw, "Frequency Stability of a Brillouin Fiber Ring Laser," J. Lit. Technol. **13**(7), 1445–1451 (1995).
22. P. Nicati, K. Toyama, S. Huang, and H. J. Shaw, "Frequency Pulling in a Brillouin Fiber Ring Laser," IEEE Photonic. Tech. L. **6**(7), 801–803 (1994).
23. C. A. López-Mercado, V. V. Spirin, S. I. Kablukov, E. A. Zlobina, I. O. Zolotovskiy, P. Mégret, and A. A. Fotiadi, "Accuracy of single-cut adjustment technique for double resonant Brillouin fiber lasers," Opt. Fiber Technol. **20**(3), 194–198 (2014).
24. V. V. Spirin, C. A. López-Mercado, S. I. Kablukov, E. A. Zlobina, I. O. Zolotovskiy, P. Mégret, and A. A. Fotiadi, "Single cut technique for adjustment of doubly resonant Brillouin laser cavities," Opt. Lett. **38**(14), 2528–2530 (2013).
25. S. Norcia, S. Tonda-Goldstein, D. Dolfi, J.-P. Huignard, and R. Frey, "Efficient single-mode Brillouin fiber laser for low-noise optical carrier reduction of microwave signals," Opt. Lett. **28**(20), 1888–1890 (2003).
26. J. Geng, S. Staines, Z. Wang, J. Zong, M. Blake, and S. Jiang, "Highly Stable Low-Noise Brillouin Fiber Laser with Ultranarrow Spectral Linewidth," IEEE Photonics Technol. Lett. **18**(17), 1813–1815 (2006).
27. D. Derickson, *Fiber optic test and measurement* (Prentice Hall, 1998).

Optics EXPRESS

28. S. Shin, U. Sharma, H. Tu, W. Jung, and S. A. Boppart, "Characterization and analysis of relative intensity noise in broadband optical sources for optical coherence tomography," IEEE Photonics Technol. Lett. **22**(14), 1057–1059 (2010).
29. J. Geng and S. Jiang, "Pump-to-Stokes transfer of relative intensity noise in Brillouin fiber ring lasers," Opt. Lett. **32**(1), 11–13 (2007).
30. J. Geng, S. Staines, Z. Wang, J. Zong, M. Blake, and S. Jiang, "Actively stabilized Brillouin fiber laser with high output power and low noise," in *Proceedings of Optical Fiber Communication Conference and the National Fiber Optic Engineers Conference* (IEEE, 2006).
31. T. Horiguchi, K. Shimizu, T. Kurashima, M. Tateda, and Y. Koyamada, "Development of a distributed sensing technique using Brillouin scattering," J. Lit. Technol. **13**(7), 1296–1302 (1995).